Figure S1

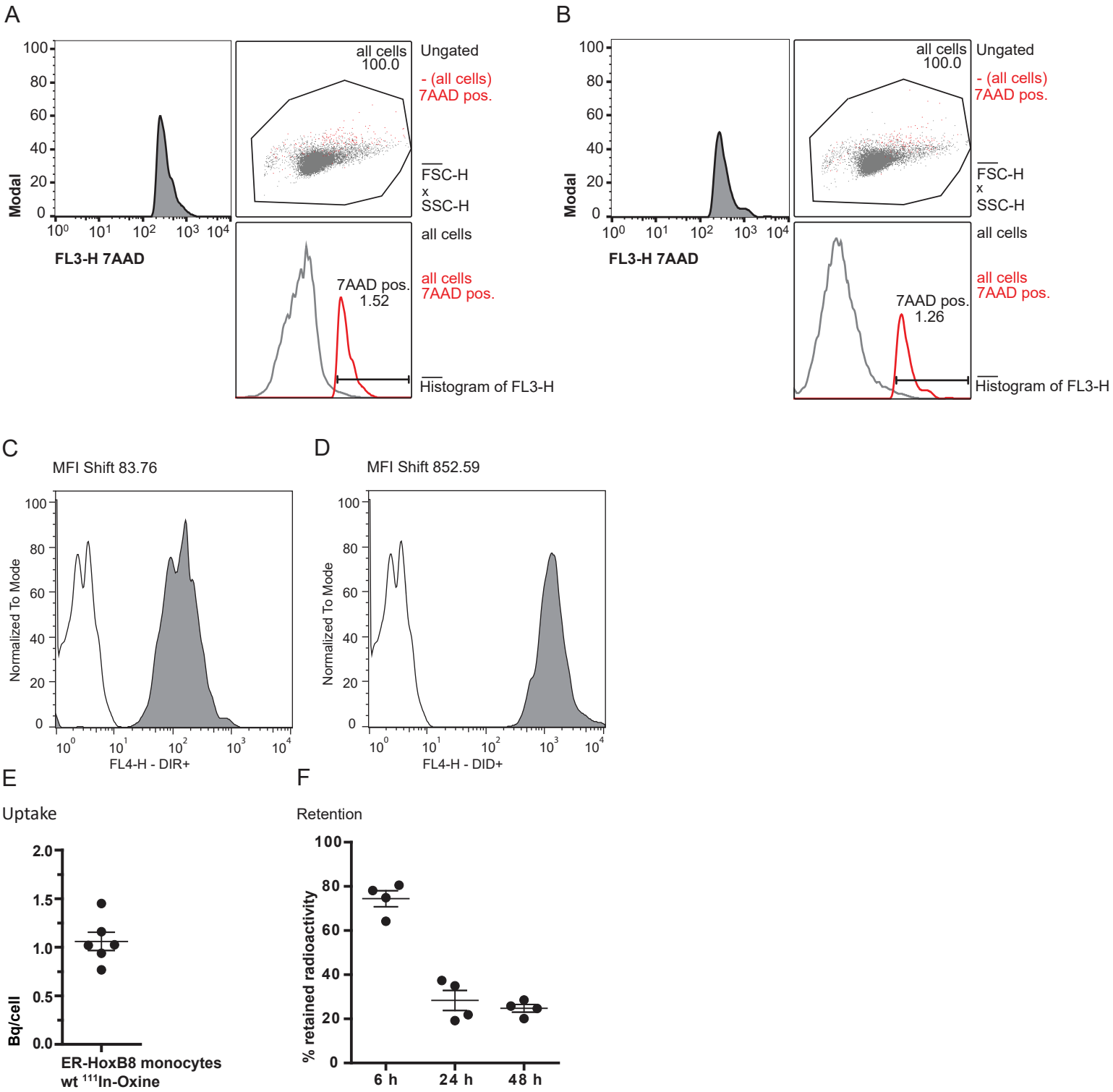
A
B
Modal
FL3-H 7AAD
all cells
100.0
Ungated
- (all cells)
7AAD pos.
FSC-H
x
SSC-H
all cells
all cells
7AAD pos.
7AAD pos.
1.52
7AAD pos.
1.26
Histogram of FL3-H
C
D
MFI Shift 83.76
MFI Shift 852.59
Normalized To Mode
FL4-H - DIR+
FL4-H - DID+
E
F
Uptake
Retention
Bq/cell
ER-HoxB8 monocytes
wt 111In-Oxine
% retained radioactivity
6 h
24 h
48 h

Figure S2

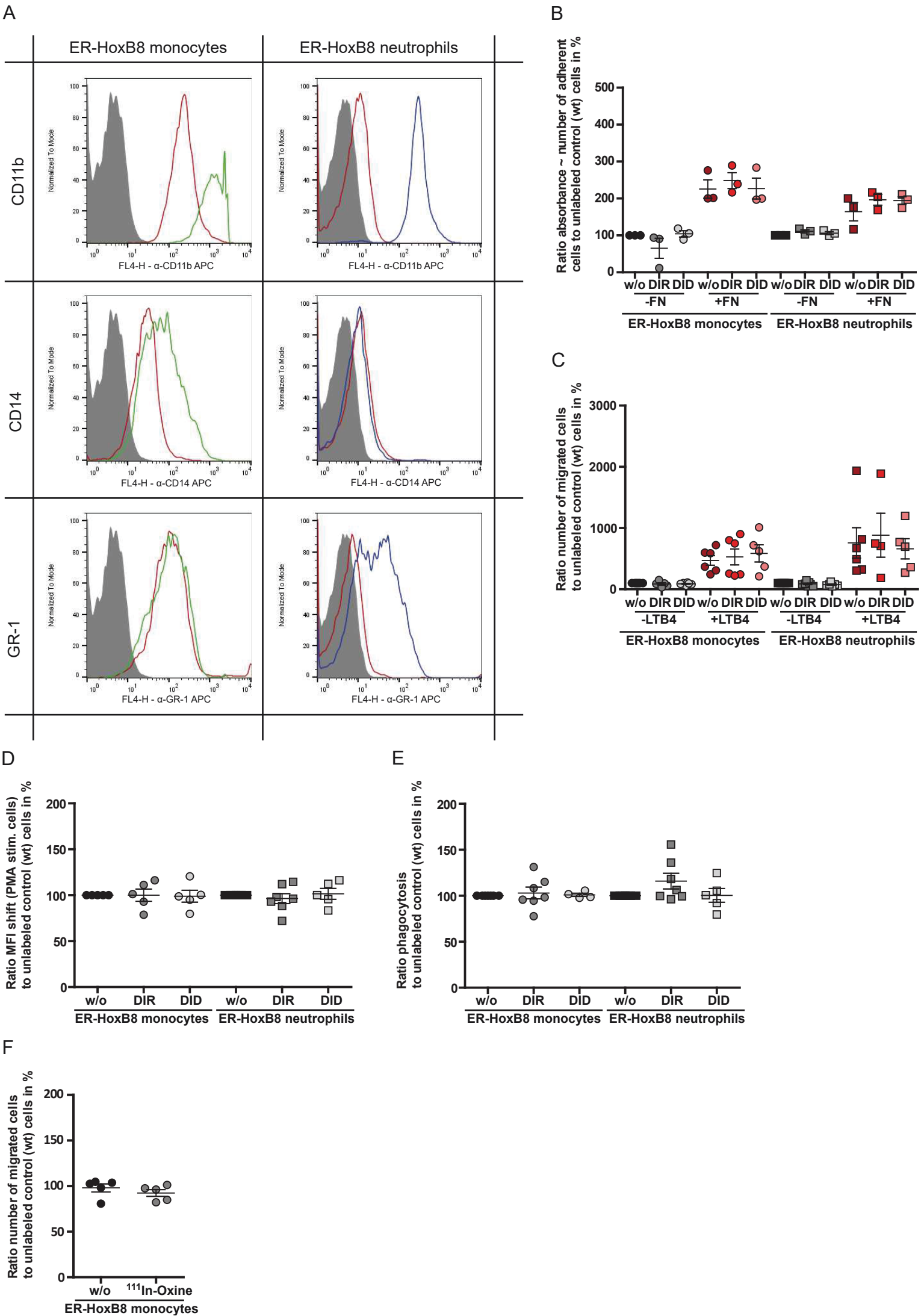
A
ER-HoxB8 monocytes
ER-HoxB8 neutrophils
CD11b
CD14
GR-1
Normalized To Mode
FL4-H - α-CD11b APC
FL4-H - α-CD14 APC
FL4-H - α-GR-1 APC
B
Ratio absorbance ~ number of adherent cells to unlabeled control (wt) cells in %
w/o DIR DID w/o DIR DID w/o DIR DID w/o DIR DID
-FN +FN -FN +FN
ER-HoxB8 monocytes
ER-HoxB8 neutrophils
C
Ratio number of migrated cells to unlabeled control (wt) cells in %
w/o DIR DID w/o DIR DID w/o DIR DID w/o DIR DID
-LTB4 +LTB4 -LTB4 +LTB4
ER-HoxB8 monocytes
ER-HoxB8 neutrophils
D
Ratio MFI shift (PMA stim. cells) to unlabeled control (wt) cells in %
w/o DIR DID w/o DIR DID
ER-HoxB8 monocytes
ER-HoxB8 neutrophils
E
Ratio phagocytosis to unlabeled control (wt) cells in %
w/o DIR DID w/o DIR DID
ER-HoxB8 monocytes
ER-HoxB8 neutrophils
F
Ratio number of migrated cells to unlabeled control (wt) cells in %
w/o 111In-Oxine
ER-HoxB8 monocytes

Figure S3

A

ER-HoxB8 monocytes wt $^{111}$In-Oxine

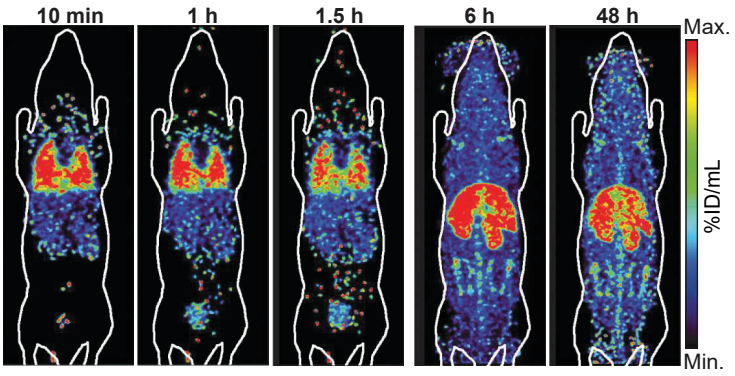


B

ER-HoxB8 monocytes wt $^{111}$In-Oxine

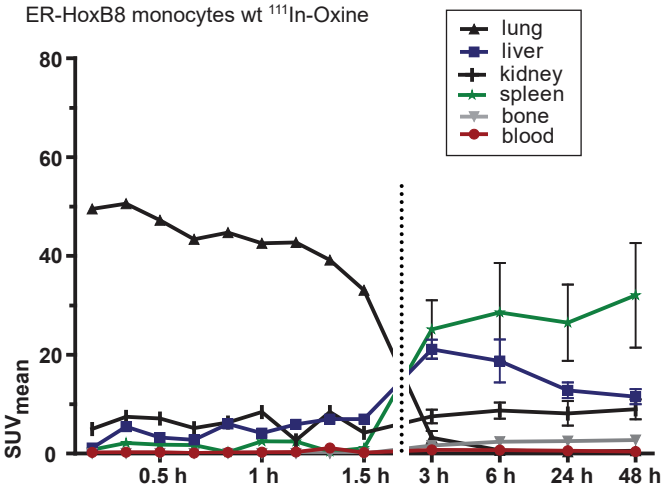

Figure S4

A

One color imaging

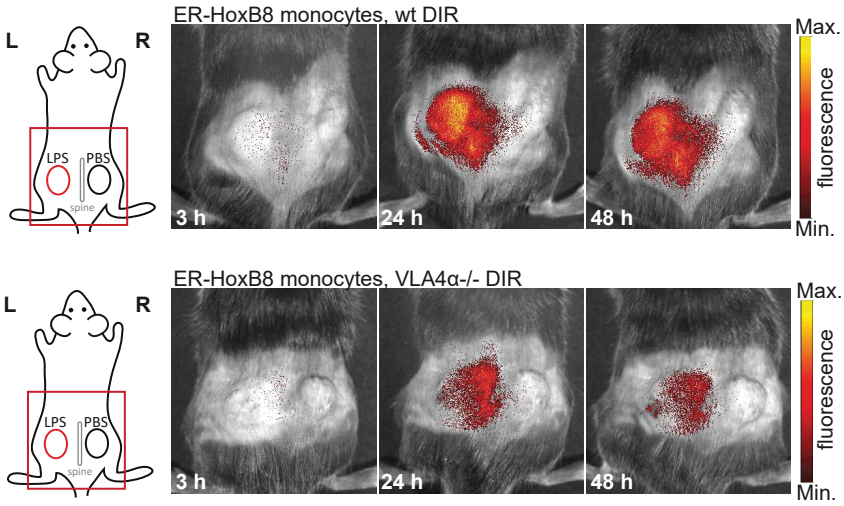


B

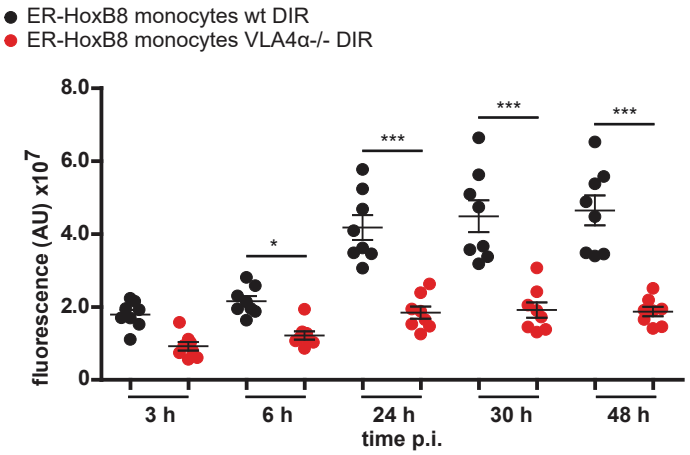

Figure S5

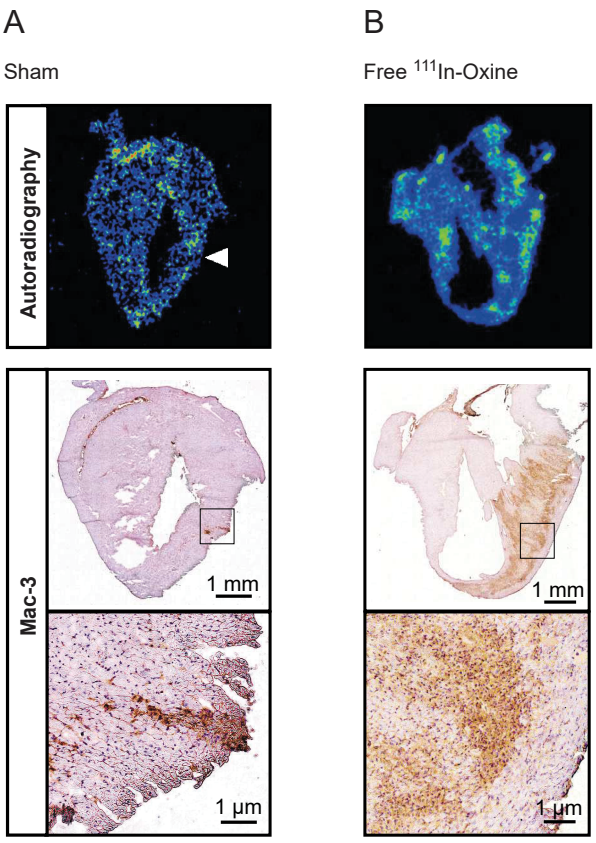
A
Sham
B
Free $^{111}$In-Oxine
Autoradiography
Mac-3
1 mm
1 µm
1 mm
1 µm

**Figure S1: Flow cytometry analysis of viability and labeling efficiency of DIR and DID labeled ER-HoxB8 monocytes and uptake and retention of $^{111}$In-Oxine labeled ER-HoxB8 monocytes.**
ER-HoxB8 *wildtype (wt)* monocytes were labeled with DIR or DID (A-D) and $^{111}$In-Oxine, respectively (E-F). (A) 7-Aminoactinomycin (7AAD) staining for living/dead cells after DIR labeling procedure. 7AAD positive cells can be detected in FL3-H. (B) 7AAD staining for living/dead cells after DID labeling procedure. 7AAD positive cells can be detected in FL3-H. (C) Labeling efficiency (MFI Shift) for DIR labeling. Labeled cells can be detected in FL4-H. (D) Labeling efficiency for DID labeling. Labeled cells can be detected in FL4-H. (E) Absolute uptake of $^{111}$In-Oxine into ER-HoxB8 monocytes (n=6 independent experiments). (F) Retention of radioactivity after 6 h, 24 h and 48 h of culturing labeled cells (n=4 independent experiments). (A-D) Representative histograms depicted, open graphs represent unlabeled control cells, solid grey graphs represent DIR/DID labeled ER-HoxB8 cells. (E-F) Data shown as dotplots with mean ± SEM, retention data (F) was corrected for radioactive decay.

**Figure S2: *In vitro* functional assays of labeled ER-HoxB8 *wildtype* monocytes and neutrophils.**
ER-HoxB8 *wildtype* progenitor cells were differentiated to monocytes (GM-CSF) or neutrophils (SCF). (A) Representative flow cytometry analysis of surface marker expression of undifferentiated/ differentiated monocytic or neutrophilic cells. Tinted grey histograms: isotype control, open histograms: red: day 0, blue: differentiated neutrophils, green: differentiated monocytes. Differentiated cells were labeled with DIR/DID (B-E) or $^{111}$In-Oxine (F) or left untreated. Cell functionality was checked by (B) adhesion-, (C, F) transwell migration-, (D) ROS production- and (E) phagocytosis assay. (B) Adhesion of labeled ER-HoxB8 monocytes/neutrophils on plastic surface with or w/o fibronectin (25 µg/mL) as compared to unlabeled control cells (n=3 independent experiments). (C) Transwell migration of labeled ER-HoxB8 monocytes/neutrophils with or w/o LTB4 (12 nM) stimulation as compared to unlabeled control cells (Mono *wt* DIR: n=5, Mono *wt* DID: n=6, Mono *wt* LTB4: n=6, Mono *wt* DIR LTB4: n=6, Mono *wt* DID LTB4: n=5, Neutro *wt* DIR: n=7, Neutro *wt* DID: n=7, Neutro *wt* LTB4: n=6, Neutro *wt* DIR LTB4: n=4, Neutro *wt* DID LTB4: n=5 independent experiments). (D) ROS production of labeled ER-HoxB8 monocytes/neutrophils after PMA stimulation (100 nM) as compared to unlabeled control cells shown as ratio of MFI shifts of FL1-H (Mono: n=5, Neutro *wt*: n=7, Neutro *wt* DIR: n=7, Neutro *wt* DID: n=5 independent experiments). (E) Phagocytosis of latex beads of labeled ER-HoxB8 monocytes/neutrophils as compared to unlabeled control cells (Mono *wt*: n=7, Mono *wt* DIR: n=7, Mono *wt* DID: n=4, Neutro *wt*: n=7, Neutro *wt* DIR: n=7, Neutro *wt* DID: n=5 independent experiments). (F) Transwell migration of labeled ER-HoxB8 monocytes as compared to unlabeled control cells (n=5 independent experiments). Data shown as dotplots with mean ± SEM, normalized to untreated, unlabeled ER-HoxB8 *wt* monocytes or neutrophils (set as 100 %).

**Figure S3: Whole-body biodistribution dynamics of $^{111}$In-Oxine labeled ER-HoxB8 *wildtype* monocytes in healthy mice.**
ER-HoxB8 *wildtype* cells were labeled with $^{111}$In-Oxine, injected in healthy C57 BL/6 mice and their distribution was analyzed by SPECT imaging over the first 90 min, 3 h, 6 h, 24 h and 48 h (90 min: n=1, 3 h: n=3, 6 h: n=4, 24 h/48 h: n=5 independent experiments) p.i. Images show maximum intensity projections. Data is displayed as mean ± SD. SUV = standardized uptake units.

**Figure S4: *In vivo* one color imaging of *wt* and *VLA4α-/-* monocyte migration in a CG model.**
ER-HoxB8 *wildtype* and *VLA4α-/-* monocytes were labeled with DIR and each cell population was injected in an individual animal (A-B). FRI images were taken 0 h, 3 h, 6 h, 24 h, 30 h and 48 h p.i. (A) Representative imaging series of one color imaging approach in two individual mice 3 h-48 h p.i. Upper panel shows LPS plug infiltration of ER-HoxB8 *wt* monocytes (DIR). Lower panel shows LPS plug infiltration of *VLA4α-/-* monocytes (DIR). (B) Statistical analysis of imaging of ER-HoxB8 *wt* or *VLA4α-/-* cell migration to LPS plug (left) corresponding to experimental setting in (A) (n=8 mice, 3 independent experiments). Images orientation: L = left, R = right, fluorescence = fluorescence intensity (AU). Data shown as dotplot with mean ± SEM, corrected to baseline and labeling efficiency. Statistical significance was calculated using 2-way ANOVA and Bonferroni posttests comparing ER-HoxB8 *wildtype* and *VLA4α-/-* cells: *$p < 0.05$, **$p < 0.01$, ***$p < 0.001$.

**Figure S5: Migration of $^{111}$In-Oxine labeled ER-HoxB8 *wildtype* monocytes in sham operated animals and distribution of free labeling agents in myocardial infarction.** (A) ER-HoxB8 *wildtype* cells were labeled with $^{111}$In-Oxine and injected 1 day after sham surgery. Autoradiographic analysis shows no specific signal from $^{111}$In-Oxine labeled cells. Immunohistochemical staining for Mac-3 revealed positive cells only at the site of ligation. (B) Free $^{111}$In-Oxine was injected 1 day after coronary artery ligation. Representative autoradiographic image showing no specific accumulation of free $^{111}$In-Oxine in the infarct zone. On histological slides α-Mac-3 staining defines the area of infarction and was clearly distinguishable from the remote myocardial tissue by its broad positive Mac-3 signal.